



OPEN

Computational fluid dynamics comparison of prevalent liquid absorbents for the separation of SO₂ acidic pollutant inside a membrane contactor

Yan Cao¹, Ali Taghvaie Nakhjiri^{2✉} & Mahdi Ghadiri^{3,4}

In recent years, the emission of detrimental acidic pollutants to the atmosphere has raised the concerns of scientists. Sulphur dioxide (SO₂) is a harmful greenhouse gas, which its abnormal release to the atmosphere may cause far-ranging environmental and health effects like acid rain and respiratory problems. Therefore, finding promising techniques to alleviate the emission of this greenhouse gas may be of great urgency towards environmental protection. This paper aims to evaluate the potential of three novel absorbents (seawater (H₂O), dimethyl aniline (DMA) and sodium hydroxide (NaOH) to separate SO₂ acidic pollutant from SO₂/air gaseous stream inside the hollow fiber membrane contactor (HFMC). To reach this goal, a CFD-based simulation was developed to predict the results. Also, a mathematical model was applied to theoretically evaluate the transport equations in different compartments of contactor. Comparison of the results has implied seawater is the most efficient liquid absorbent for separating SO₂. After seawater, NaOH and DMA are placed at the second and third rank (99.36% separation using seawater > 62% separation using NaOH > 55% separation using DMA). Additionally, the influence of operational parameters (i.e., gas and liquid flow rates) and also membrane/module parameters (i.e., length of membrane module, hollow fibers' number and porosity) on the SO₂ separation percentage is investigated as another highlight of this paper.

In recent years, combustion of fossil fuels is known as one of the momentous reasons of human-based greenhouse gases emission to the atmosphere¹⁻³. Sulphur dioxide (SO₂) is an important greenhouse gas, which its release into the atmosphere may result in various adverse effects on human health and ecosystem including respiratory problems, asthma attacks, urban smog and acid rain^{4,5}. By the emission of this acidic gas to the atmosphere, sulfur trioxide (SO₃) and sulfuric acid (H₂SO₄) are generated, which can be known as the secondary source of pollutants. The abnormal deposition of these secondary contaminants causes the acidification of water sources and damages agricultural crops^{6,7}. Therefore, the separation of these detrimental pollutants has found paramount importance due to the legislation of strict environmental regulations all over the world^{8,9}.

Membrane-based gas absorption using microporous hollow fiber membrane contactor (HFMC) is known as a trustworthy alternative for prevalent separation processes of greenhouse gases such as cryogenic distillation, packed bed tower, spray tower and adsorption¹⁰⁻¹⁴. HFMCs have been recently of great interest as a mass transfer device due to having disparate advantages like constant interfacial areas, flexibility of operation, and simplicity of scale-up and independent adjustment of gas/liquid streams¹⁵⁻¹⁸. The important role of membrane materials in the separation of acidic pollutants is incontrovertible. In recent years, polypropylene (PP), polyvinylidene fluoride (PVDF), polyether sulfone (PSf) and polytetrafluoroethylene (PTFE) are among the most commonly-employed materials for fabricating hydrophobic membranes^{13,19-23}. True selection of chemical absorbent is an important responsibility of researchers and scientists to improve the efficiency of greenhouse gases separation. The existence

¹School of Computer Science and Engineering, Xi'an Technological University, Xi'an 710021, People's Republic of China. ²Department of Petroleum and Chemical Engineering, Science and Research Branch, Islamic Azad University, Tehran, Iran. ³Institute of Research and Development, Duy Tan University, Da Nang 550000, Vietnam. ⁴The Faculty of Environment and Chemical Engineering, Duy Tan University, Da Nang 550000, Vietnam. ✉email: taghvaiali@yahoo.com

of some advantages such as eco-friendliness, suitable selectivity, excellent efficiency and reasonable cost may increase the popularity of a liquid absorbent for using in the membrane-based gas absorption processes^{14,24}.

CFD is a new branch of science, which possesses great capability to predict the fluid-flow phenomena on the basis of the conservation laws^{25–27}. Due to the indisputable benefit of the CFD approach for different process industries, its rapid advancement and vast utilizations have taken place during the recent decades^{28,29}. Continuous development of CFD tools and its growing ability to predict the results with lower costs have significantly increased the popularity of this approach among the researchers of different scientific scopes^{30–34}. In the case of membrane-based gas absorption process, the application of CFD technique to analyze the principal transport equations through disparate sides of HFMC has been a promising alternative to decrease the cost of experimental investigations^{35–37}.

In an interesting study, Ariono et al. employed PP membrane contactor for the separation of SO₂ from flue gas. Based on their simulation results, Na₂SO₃ aqueous solution was introduced as a promising liquid absorbent and could 1.8 times improve the absorption flux of SO₂ acidic gas compared to water³⁸. In another investigation, Kong et al. numerically analyzed the mass transfer performance of a ceramic HFMC for the separation of post-combustion SO₂ from flue gas using NaOH alkali absorbent. They concluded that at a constant gas velocity (500 mm.s⁻¹) and SO₂ concentration (0.041 mol.m⁻³), increment in the concentration of NaOH from 0.2 to 1.5 mol. L⁻¹ significantly enhanced the SO₂ flux from 0.1 to about 0.55 mol.m⁻² h⁻¹³⁹.

This article aims to develop a numerical simulation based on the CFD and finite element (FE) techniques to predict the separation percentage of SO₂ greenhouse gas from a gaseous flow containing SO₂ and air inside the HFMC. As the novelty, three liquid absorbents (dimethyl aniline (DMA), sodium hydroxide (NaOH) and seawater (H₂O)) are compared with each other and the most effective one is introduced. Ultimately, investigating the effect of important operational and also membrane/module parameters on the SO₂ separation is investigated as another highlight of this research paper.

Reaction mechanism of SO₂ in different absorbents

The ball-and-stick molecular structure of employed liquid absorbents (DMA, NaOH and H₂O) is presented in Fig. 1.

The chemical absorption of SO₂ acidic contaminant in H₂O absorbent takes place by a hydrolysis reaction, presented by the equilibriums 1 to 4⁷.

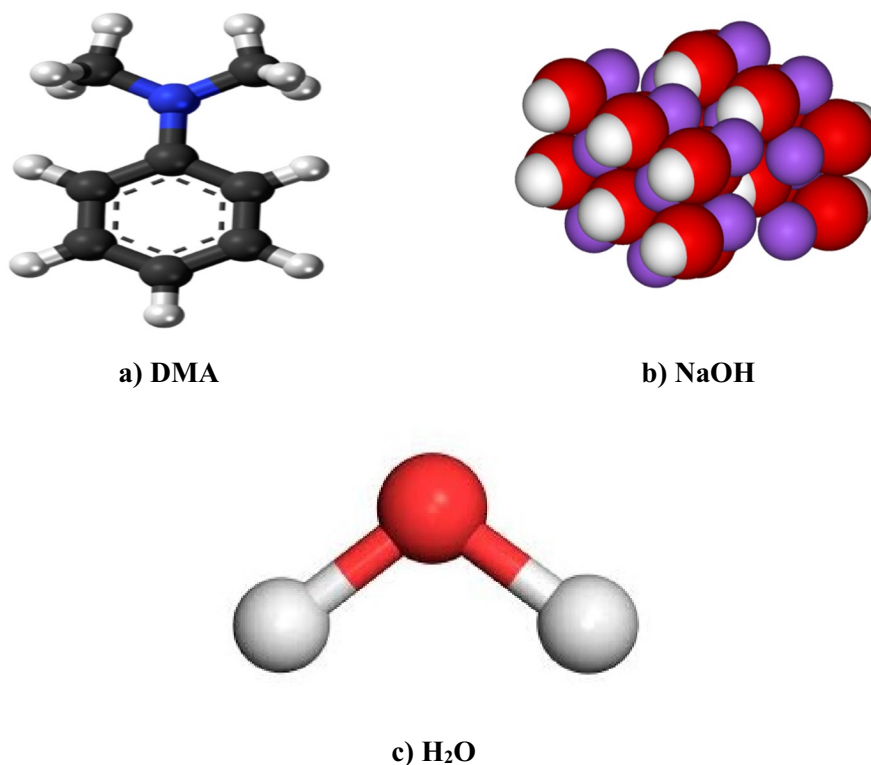


Figure 1. Ball-and-stick molecular structure of employed liquid absorbents^{40–42}.



Seawater can be considered as a complex system, which includes disparate dissolved chemical components like Na^+ , Mg^{2+} , Ca^{2+} , K^+ , SO_4^{2-} and HCO_3^- and Br^- . These components contain more than 95% of dissolved salt in seawater. Additionally, NaCl has a significant value in seawater and occupies nearly 85% of the constant component⁸. The existed carbonate system in the seawater can be obviously described by the following equilibriums^{18,43,44}:

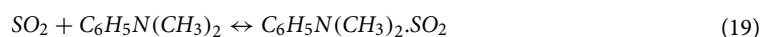


According to the abovementioned equilibriums, seawater possesses great potential for the absorption of SO_2 acidic pollutant. The presence of complex CO_2 - H_2O - HCO_3^- - CO_3^{2-} equilibrium system eventuates in increasing the mass transfer performance of SO_2 acidic pollutant in the seawater, which positively encourages its removal.

In the case of SO_2 separation using DMA liquid absorbent, the following reactions take place⁴⁵:



Moreover, formation of an additional compound occurs during the SO_2 - DMA reaction as follows⁴⁶:



The separation process of SO_2 acidic pollutant in the NaOH occurs by the following equilibrium⁴⁷:



Modeling

HFMC is a novel apparatus, which is designed to carry out the separation process using a hydrophobic microporous membrane⁴⁸. Employed membrane in a gas-liquid HFMC is usually applied as a gas-liquid interface and provide better chance for efficient contact between two phases without direct mixing^{49,50}. Great selectivity of the HFMC is due to the existence of gradient between the components' solubility in the liquid phase. Thus, the majority of commercial HFMC apply microporous membranes due to having higher mass transfer properties⁵¹. Figure 2 schematically shows the gas-liquid interface inside a microporous HFMC.

Through each HFMC, the gas-liquid mass transfer process takes place via the mechanism of solution diffusion inside the micropores of a hydrophobic membrane. Figure 3 schematically presents the two-dimensional (2D) illustration of SO_2 mass transfer inside different domains (shell, membrane and tube) of HFMC.

As can be seen in Fig. 3, gaseous mixture including SO_2 air flows in the shell side from up to down (from $z=L$ to $z=0$) and H_2O , DMA and NaOH liquid absorbents move in the tube side from down to top (from $z=0$ to $z=L$).

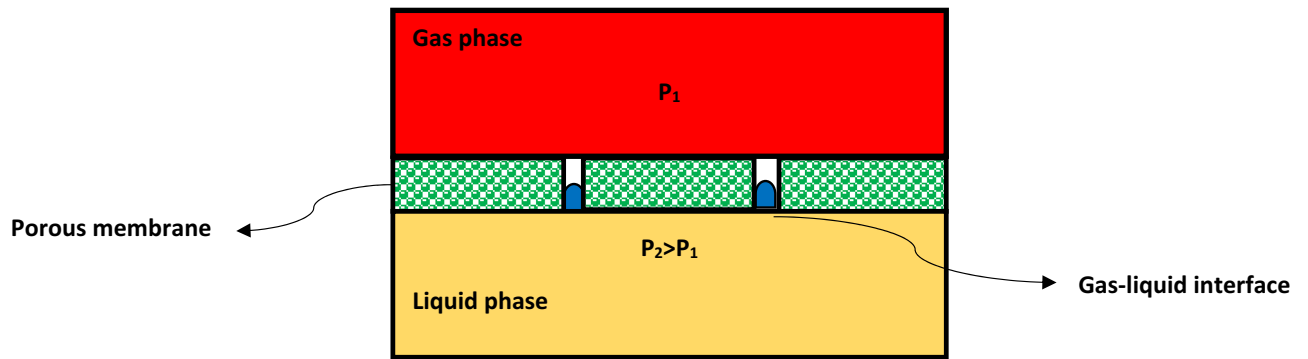


Figure 2. Schematic depiction of gas–liquid interface inside a microporous HFMC.

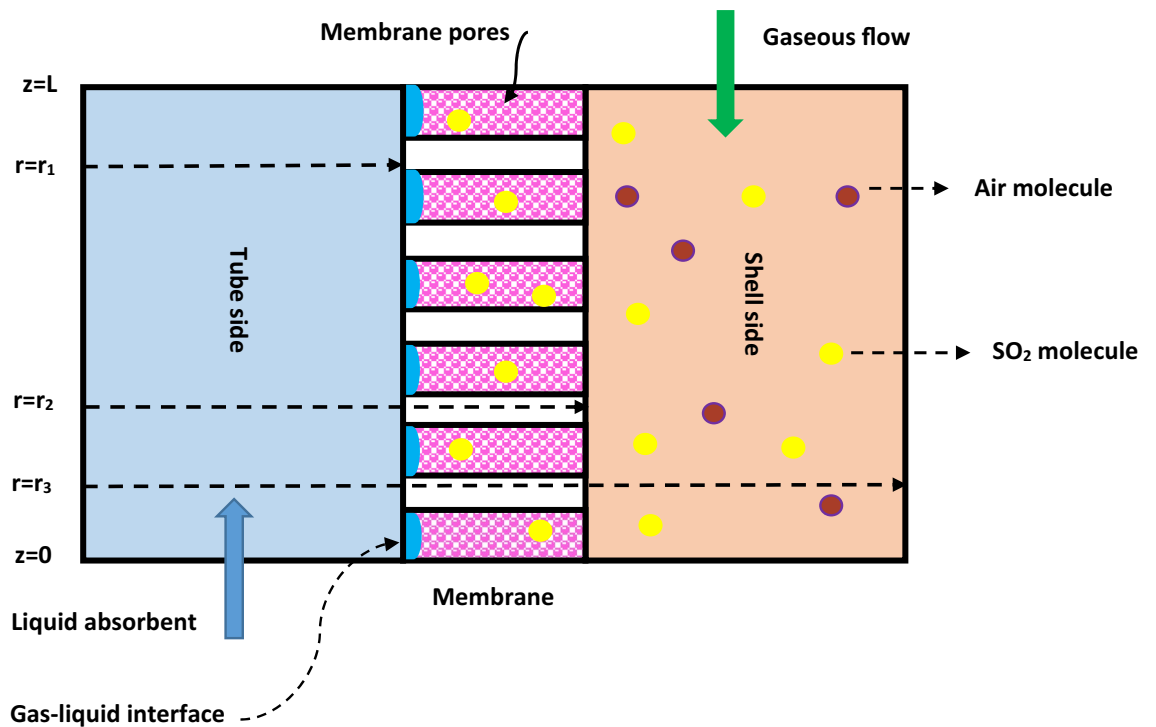


Figure 3. 2D depiction of SO₂ mass transfer inside different domains of contactor.

No	Assumption
1	Steady state operation
2	Non-wetting mode in membrane (micropores is only filled with gas molecules)
3	Isothermal condition of gas and liquid streams
4	The use of Happel's free surface model for approximating the assumptive radius of shell around each fiber
5	Ideal behavior of gas and liquid absorbent
6	Hydrophobicity nature of employed membrane
7	Laminar flow regime in both tube and shell
8	The use of Henry's law in the membrane-liquid contact interface

Table 1. Applied assumptions to develop the simulation^{52–57}.

$z = L$), counter-currently. The employed assumptions to implement the mathematical modeling and 2D simulation is presented in Table 1.

COMSOL Multiphysics is as an attractive CFD-based software with brilliant capability to solve partial differential equations with different stiff/non-stiff boundary and initial conditions. In this paper, PDEs of mass and momentum are solved using this robust software based on CFD approach. To solve PDEs of mass and momentum, COMSOL Multiphysics version 6 was installed on a 64-bit platform with an Intel(R) core (TM) i7-10510U CPU and a 16 Gigabyte RAM. The needed time for solving the PDEs and present the results was about 20 s. Moreover, with the aim of managing the material balance error during the solution of mass/momentum PDEs, PARDISO numerical solver was employed owing to its brilliant advantages like excellent memory performance and robustness^{58,59}. The principal PDEs of mass and momentum in tube, membrane and shell sides are presented in Table 2.

In Table 2, $D_{SO_2,s}$, $D_{SO_2,mem}$ are defined as the diffusion coefficient of SO_2 greenhouse gas in the shell and membrane. Also, $D_{i,t}$ is the diffusion coefficient of i (SO_2 , H_2O , $NaOH$ and DMA) in the tube. Additionally, $V_{z,s}$, $V_{z,t}$, \bar{V}_s , \bar{V}_t and C are described as the shell's velocity in axial direction, tube velocity in the axial direction, the average velocity in the shell, the average velocity inside the tube and concentration, respectively. Boundary conditions at each main domains of HFMC are presented in Table 3.

The required parameters of microporous membrane and module following with important physicochemical properties of SO_2 acidic pollutants and seawater, $NaOH$ and DMA liquid absorbents are rendered in Table 4.

Results and discussion

Validation of developed modeling and 2D simulation. Up to our knowledge, very few papers experimentally evaluated the performance of $NaOH$, DMA and H_2O to separate SO_2 acidic pollutant. Therefore, the validation of developed 2D simulation was performed via the comparison of simulation outcomes with experimental results obtained by Karoor and Sirkar about the separation of SO_2 using pure water⁶³. As demonstrated in Fig. 4, there is a favorable agreement between the experimental data and predicted results achieved by 2D simulation, which corroborates the accuracy and validation of employed modeling and simulation in this work.

With the aim of ensuring the accuracy of developed model outcomes, the second validation was implemented via the comparison of simulation results with obtained experimental data from Xu et al. for the separation of SO_2 using $NaOH$ solution⁷². As can be seen in Fig. 5, an excellent agreement is again demonstrated between the experimental data and predicted results with the absolute relative deviation (ARD) of about 4%, which certainly corroborates the validation of developed model.

Axial concentration gradient of SO_2 . Figures 6a, 6b and 6c show the axial concentration profile of SO_2 greenhouse gas in the shell and membrane sides of the contactor, respectively. The SO_2 /air gaseous mixture

Mass transfer equation		
Domain	Tube	$D_{i,t} \left[\frac{\partial^2 C_{i,t}}{\partial r^2} + \frac{1}{r} \frac{\partial C_{i,t}}{\partial r} + \frac{\partial^2 C_{i,t}}{\partial z^2} \right] + R_i = V_{z,t} \frac{\partial C_{i,t}}{\partial z}$ (21)
	Shell	$D_{SO_2,s} \left[\frac{\partial^2 C_{SO_2,s}}{\partial r^2} + \frac{1}{r} \frac{\partial C_{SO_2,s}}{\partial r} + \frac{\partial^2 C_{SO_2,s}}{\partial z^2} \right] = V_{z,s} \frac{\partial C_{SO_2,s}}{\partial z}$ (22)
	Membrane	$D_{SO_2,mem} \left[\frac{\partial^2 C_{SO_2,mem}}{\partial r^2} + \frac{1}{r} \frac{\partial C_{SO_2,mem}}{\partial r} + \frac{\partial^2 C_{SO_2,mem}}{\partial z^2} \right] = 0$ (23)
Momentum equation		
Domain	Shell	$V_{z,s} = 2\bar{V}_s \left[1 - \left(\frac{r_2}{r_3} \right)^2 \right] \times \left[\frac{(r/r_3)^2 - (r_2/r_3)^2 + 2 \ln(r_2/r)}{3 + (r_2/r_3)^4 - 4(r_2/r_3)^2 + 4 \ln(r_2/r_3)} \right]$ (24)
	Tube	$V_{z,t} = 2\bar{V}_t \left[1 - \left(\frac{r}{r_1} \right)^2 \right]$ (25)

Table 2. Applied governing PDEs in different compartments of HFMC for developing the model^{60–62}.

Position	Shell	Membrane	Tube
$r = 0$	–	–	$\partial C_{SO_2,t} / \partial r = 0$
$r = r_1$	–	$C_{mem} = C_t/m$	$C_t = C_{mem} * m$
$r = r_2$	$C_s = C_{mem}$	$C_{mem} = C_s$	–
$r = r_3$	$\partial C_{SO_2,s} / \partial r = 0$	–	–
$z = 0$	$C_{SO_2,s} = C_{initial}$	Insulated	Outlet flow
$z = L$	Outlet flow	Insulated	$C_{SO_2,t} = 0$ $C_{solution,t} = C_{initial}$

Table 3. Employed boundary/initial conditions in different compartments of HFMC.

Parameter	Unit	Value	Ref
Fibers I.D	m	2.410^{-4}	63
Fibers O.D	m	310^{-4}	63
Shell O.D	m	0.457210^{-2}	63
Porosity of membrane (ϵ)	–	0.4	63
Tortuosity of membrane (τ)		2.5	63
Fiber's length (L)	m	0.18	63
Number of fibers (n)	–	75	63
$D_{SO_2,g}$	$m^2.s^{-1}$	1.2610^{-5}	64
$D_{SO_2,mem}$	$m^2.s^{-1}$	$D_{SO_2,g} (\frac{\epsilon}{\tau})$	65
D_{SO_2,H_2O}	$m^2.s^{-1}$	210^{-9}	66
$D_{SO_2,DMA}$	$m^2.s^{-1}$	2.110^{-9}	67
$D_{SO_2,NaOH}$	$m^2.s^{-1}$	2.12210^{-9}	68
m_{SO_2,H_2O}	–	25.86	69
$m_{SO_2,DMA}$	–	0.00131	70
$m_{SO_2,NaOH}$	–	0.952	71

Table 4. Membrane/module parameters and physicochemical properties of SO_2 , seawater, NaOH and DMA liquid absorbents. *ID* Inner diameter; *OD* Outer diameter.

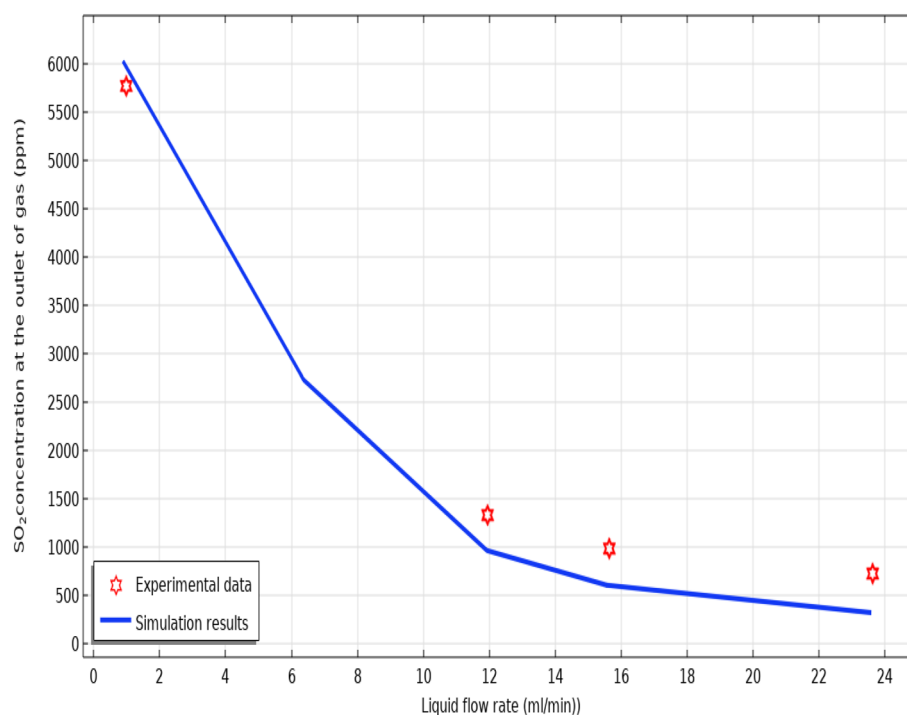


Figure 4. Validation of developed 2D simulation with experimental results. Feed gas composition: 1% SO_2 in air $T = 298$ K, $Q_g = 200$ ml min^{-1} . Experimental data was according to the study of Karoor and Sirkar⁶³.

enters to the shell side of HFMC from $z=L$, where the SO_2 concentration is maximum. On the other hand, employed liquid absorbents (NaOH, H_2O and DMA) enters to the tube compartment of contactor from $z=0$. At this location, the concentration of liquid absorbents is in the highest value and the concentration of SO_2 is considered zero. When the gaseous mixture flows inside the shell, the presence of concentration difference causes the movement of SO_2 from shell to the porous membrane. Diffusion of SO_2 molecules to the membrane micropores facilitates their contact and consequently their removal by flowing absorbents in the tube side. The results show that the dimensionless concentration of SO_2 in the shell side declines from 1 to 0.45, 0.0064 and 0.38 using DMA, seawater and NaOH, respectively. This finding proves the SO_2 separation percentage of 55, 99.36 and 62% by employing DMA, seawater and NaOH as liquid absorbents. High SO_2 separation efficiency of seawater can be owing to the presence of complex $CO_2-H_2O-HCO_3^-CO_3^{2-}$ equilibrium system, which significantly enhances its mass transfer coefficient compared to other liquid absorbents⁸.

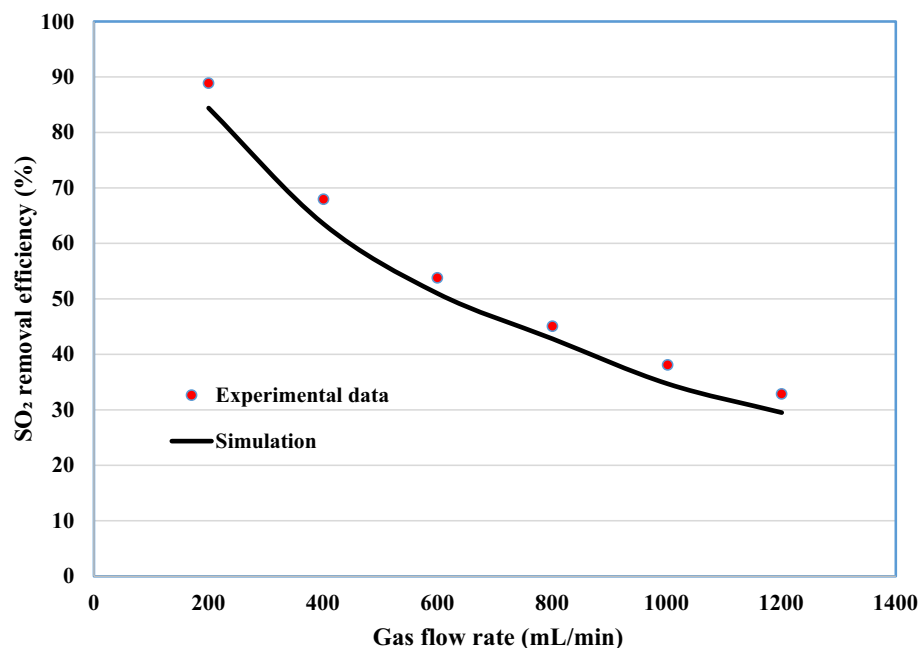


Figure 5. Validation of developed 2D simulation with experimental results. Inlet SO₂ concentration: 1000 ppm, T = 298 K, Q_l = 25 ml min⁻¹. Experimental data was according to the study Xu et al.⁷².

The role of gas and liquid flow rates on the SO₂ separation performance. Figure 7 illustrate the impact of gas flow rate on the separation yield of SO₂. As presented, increase in the flow rate of gaseous mixture considerably declines the residence time in the module. As the result, decrement of residence time destroys the suitable contact of SO₂ with liquid absorbents, which results in decreasing the separation efficacy. By looking at the figure, it is perceived that increase in the gas flow rate from 0.25 to 0.3 L/min decreases the SO₂ separation percentage from 100 to 77% using seawater, from 91 to 33% using NaOH and from 72 to 29% using DMA. Table 5 enlists the separation percentage of SO₂ from the gaseous mixture using seawater, NaOH and DMA liquid absorbents in different gas flow rates.

Additionally, the influence of liquid absorbents' flow rate on the percentage of SO₂ separation is shown in Fig. 8. By faster flowing of absorbents through the tube segment, the concentration of gas at the external surface of the hollow fiber along the length of the HFMC decreases significantly, which eventuates in greater mass transfer coefficient, superior concentration gradient at the shell-membrane interface and therefore, better SO₂ separation performance. Based on the figure, increase in the flow rate of liquid absorbents from 0.25 to 0.3 L/min improves the SO₂ separation percentage from 95 to 100% using seawater, from 53.5 to about 67.5% using NaOH and from 50 to 60% using DMA.

The separation performance of SO₂ greenhouse pollutant from SO₂/air gaseous stream applying seawater, NaOH and DMA absorbents in different gas flow rates is presented in Table 6.

Effect of membrane/module specifications on the separation performance. Figure 9 presents a schematic demonstration for evaluating the role of module length on the separation yield of SO₂ greenhouse gas. As illustrated, increase in the length of module possesses positive impact on improving the gas-absorbent residence time and contact area between two phases, which results in enhancing the separation yield of SO₂ greenhouse gas. It is observed that increase in the length of module from 0.05 to 0.3 m improves the SO₂ separation percentage from 83 to 100% using seawater, from 32.5 to about 72% using NaOH and from 25 to 66% using DMA.

The separation percentage of SO₂ from gaseous flow in different length of module is presented in Table 7.

Membrane porosity is a membrane-related parameter, which its increment may have an encouraging influence on the separation performance of various greenhouse gases. As shown in Fig. 10, increase in the porosity of polypropylene membrane from 0.1 to 0.5 cause a substantial enhancement in the removal efficacy of SO₂ greenhouse gas from 97 to 100% using seawater, from 35 to about 66% using NaOH and from 23 to 60% using DMA. This substantial increment can be justified due to this reality that increase in the porosity of membrane results in the enhancement of SO₂ diffusivity in the fiber micropores and also the deterioration of the mass transfer resistance inside the HFMC. Table 8 aims to present a data analysis about the role of porosity on increasing the separation percentage of SO₂ using employed chemical absorbents in the HFMC.

Figure 11 schematically presents the effect of hollow fibers' number on the separation of SO₂ greenhouse pollutant. As would be expected, increase in the number of microporous fibers substantially improves the gas-absorbent mass transfer interface and also their related contact area. Increase in the gas-liquid mass transfer interface and their contact area significantly increases the mass transfer coefficient of SO₂ and therefore, its

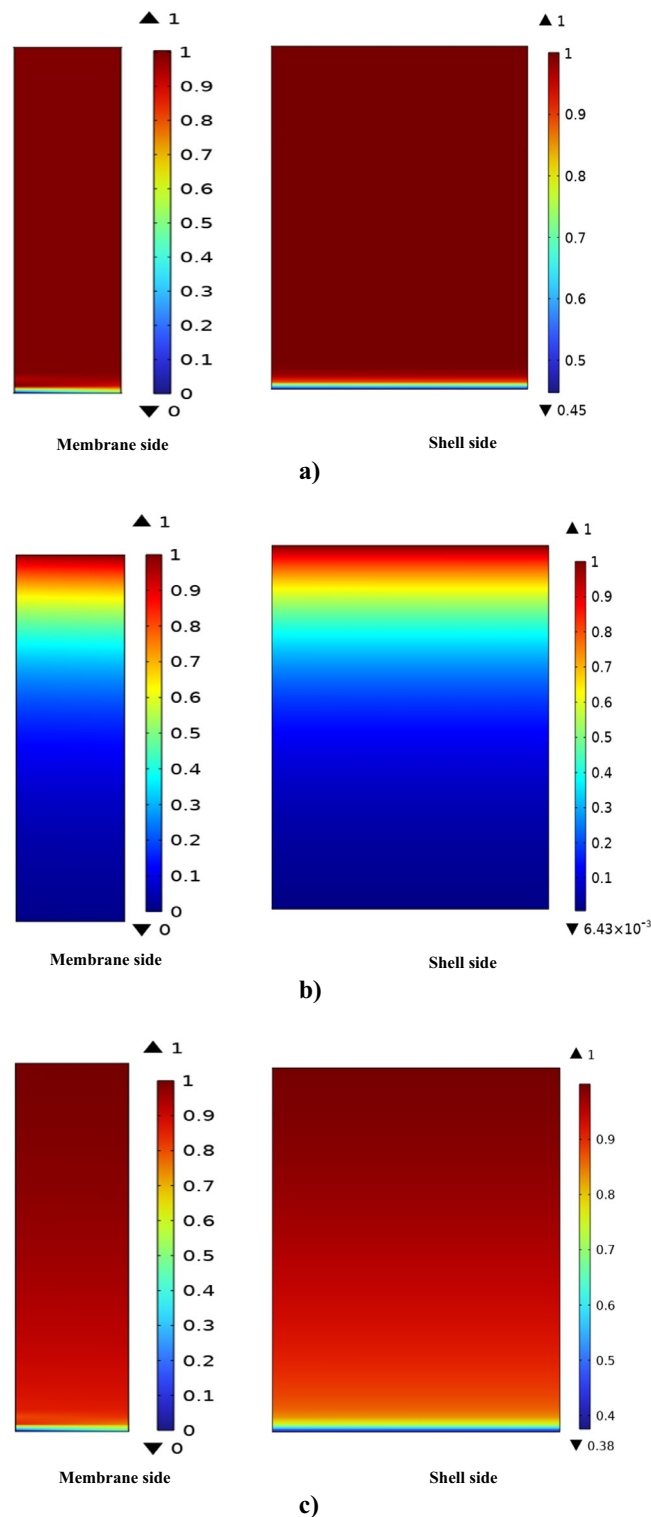


Figure 6. Axial concentration gradient of SO_2 greenhouse gas in the shell and membrane sides of the contactor using (a) DMA, (b) H_2O and (c) NaOH liquid absorbents.

separation percentage. It is demonstrated that increase in the number of fibers from 20 to 160 improves the SO_2 separation percentage from 13 to 100% using seawater, from 4 to about 96% using NaOH and from 2 to 92% using DMA.

Table 9 comprehensively presents the separation efficiency of SO_2 greenhouse contaminant in different number of hollow fibers.

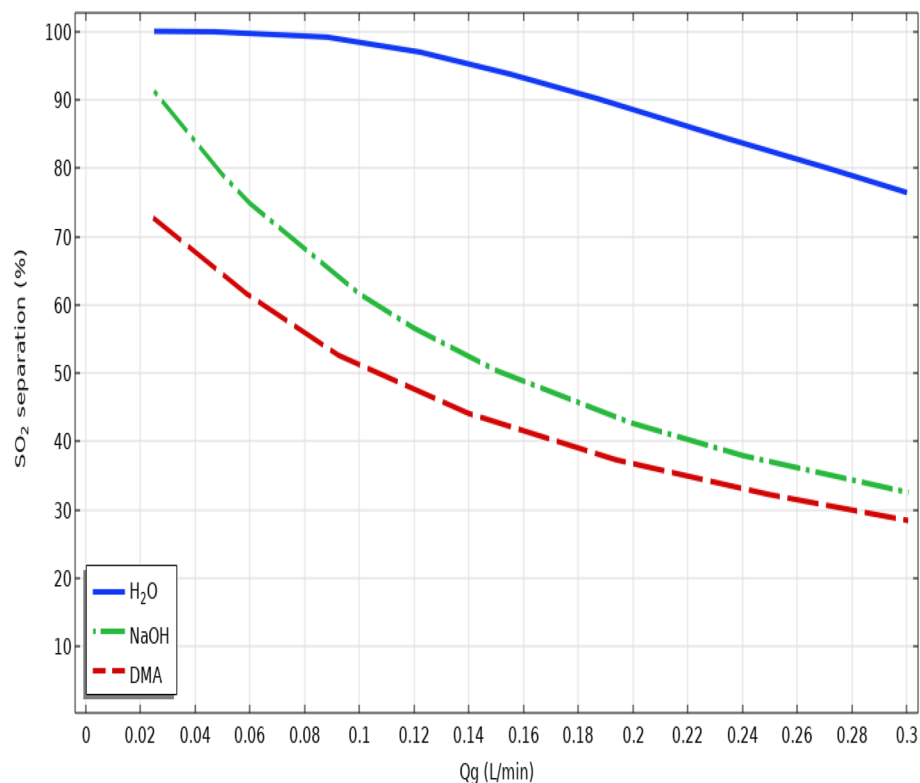


Figure 7. Effect of gas flow rate on the separation yield of SO₂ greenhouse gas.

Gas flow rate (L.min ⁻¹)	SO ₂ separation using seawater (%)	SO ₂ separation using NaOH (%)	SO ₂ separation using DMA (%)
0.025	100	91.22	72.67
0.1	98.34	61.57	51.14
0.16	93.04	48.65	42.69
0.2	88.57	42.52	36.72
0.25	82.6	37.06	32.09
0.3	76.31	32.42	28.28

Table 5. SO₂ separation percentage using seawater, NaOH and DMA liquid absorbents in disparate gas flow rates.

Conclusion

Over the last decades, industrial application of HFMCs to alleviate the extraordinary release of various greenhouse gases like SO₂ to the atmosphere has been of great attention. In this paper, the removal performance of SO₂ greenhouse contaminant from SO₂/air mixture using three novel liquid absorbents (seawater (H₂O), DMA and NaOH) was evaluated inside the HFMC. To reach this aim, a CFD-based comprehensive simulation was developed to predict the results. An FE-based mathematical model was also applied to solve the PDEs of transport in the main subdomains of contactor. The results corroborated that seawater can be recommended as the most efficacious liquid absorbent for removing SO₂ with the removal efficiency of around 99.36%. After seawater, NaOH and DMA were placed at the second and third rank with the SO₂ separation percentage of 62 and 55%, respectively (seawater (H₂O) > NaOH > DMA). Evaluation of simulation outcomes proved the deteriorative impact of gas flow rate on the SO₂ separation yield (due to decreasing the residence time of gaseous mixture in the HFMC). But, increment of other parameters like absorbent's flow rate, length of membrane module, hollow fibers' number and porosity possesses encouraging influence on the separation performance of SO₂ acidic pollutant due to declining the concentration of gaseous mixture at the external surface of hollow fibers, increasing the gas-absorbent contact area, increasing the diffusivity of SO₂ and improving the gas-liquid residence time inside the contactor, respectively.

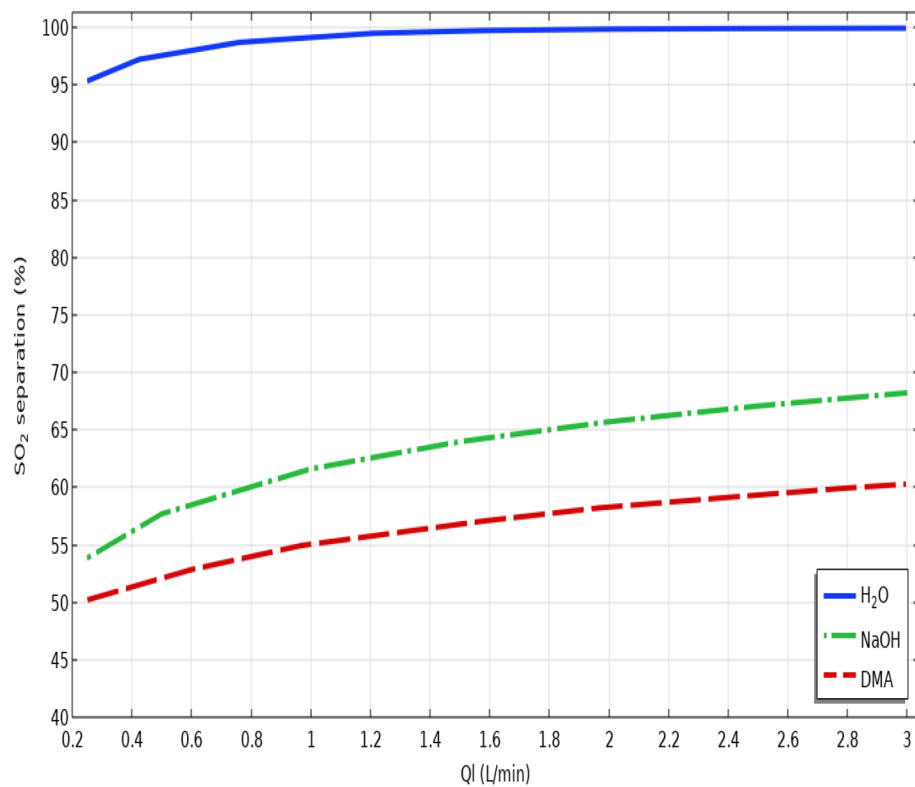


Figure 8. Effect of liquid absorbents' flow rate on the separation yield of SO₂ greenhouse gas.

Liquid flow rate (L.min ⁻¹)	SO ₂ separation using seawater (%)	SO ₂ separation using NaOH (%)	SO ₂ separation using DMA (%)
0.25	95.38	53.92	50.19
1	99.11	61.59	55.1
1.6	99.8	64.34	56.77
2	99.85	65.71	58.35
2.5	99.9	67.09	59.33
3	99.95	68.27	60.31

Table 6. SO₂ separation performance from SO₂/air gaseous stream using seawater, NaOH and DMA liquid absorbents in different liquid flow rates.

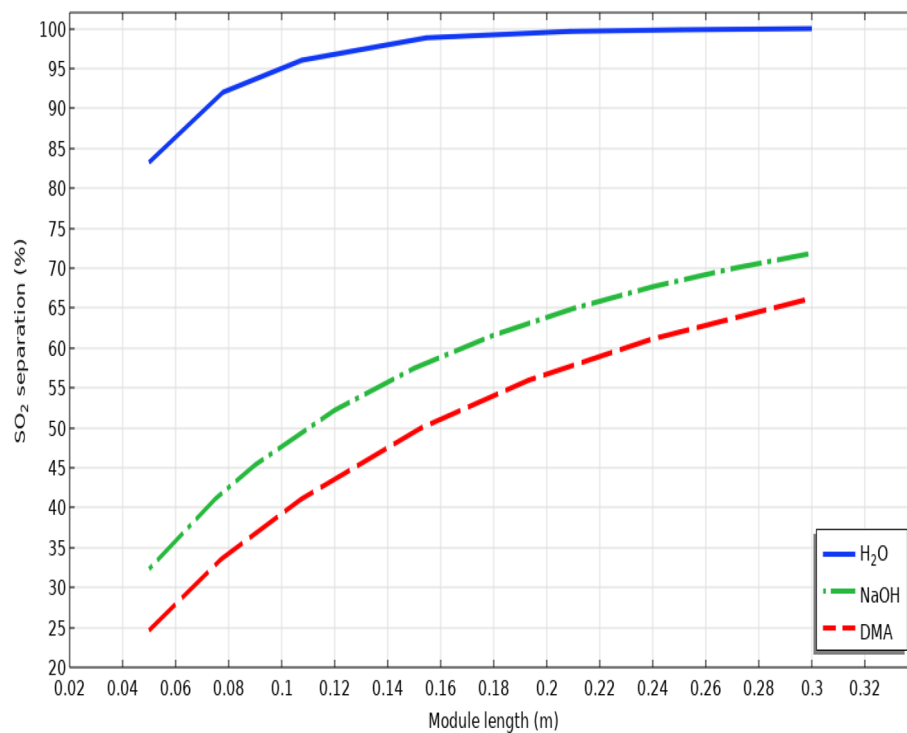


Figure 9. Effect of module length on the separation yield of SO₂ greenhouse gas.

Module length (m)	SO ₂ separation using seawater (%)	SO ₂ separation using NaOH (%)	SO ₂ separation using DMA (%)
0.05	83.14	32.3	24.54
0.15	98.52	57.45	49.56
0.2	99.46	63.87	56.65
0.25	99.73	68.42	62
0.3	99.86	71.77	66.15

Table 7. SO₂ separation performance using seawater, NaOH and DMA liquid absorbents in different lengths of module.

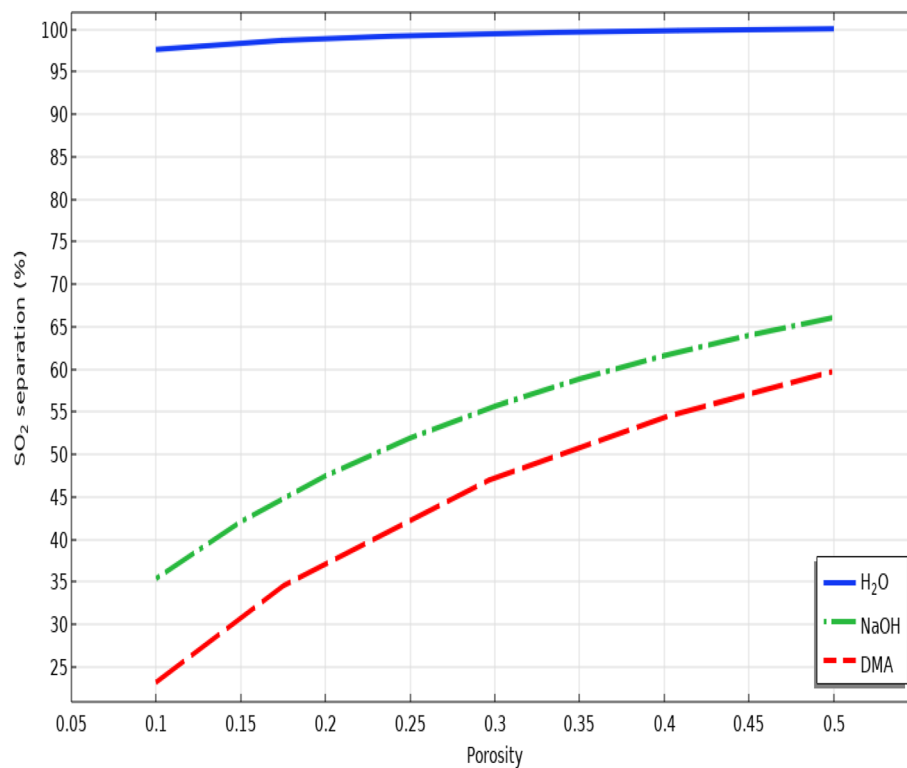


Figure 10. Effect of membrane porosity on the separation yield of SO₂ greenhouse gas.

Porosity	SO ₂ separation using seawater (%)	SO ₂ separation using NaOH (%)	SO ₂ separation using DMA (%)
0.1	96.98	18.29	3.02
0.2	98.65	33.72	20.63
0.3	99.49	43.96	33.38
0.4	100	51.51	42.28
0.5	100	57.21	49.16

Table 8. Impact of membrane porosity on the SO₂ separation performance using seawater, NaOH and DMA liquid absorbents.

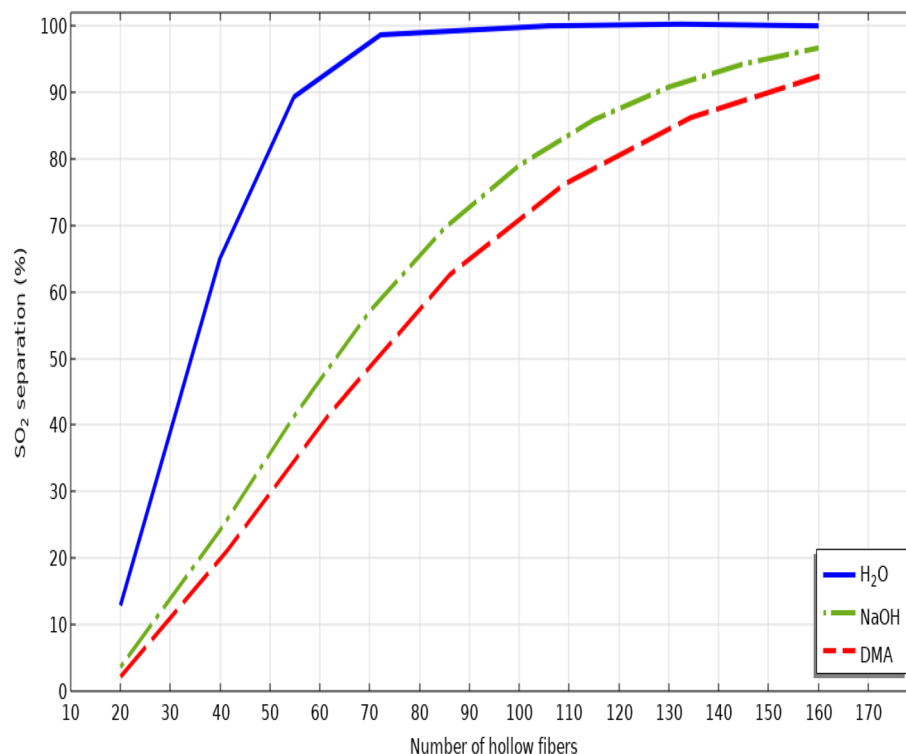


Figure 11. Effect of the number of hollow fibers on the separation yield of SO₂ greenhouse gas.

Number of fibers	SO ₂ separation using seawater (%)	SO ₂ separation using NaOH (%)	SO ₂ separation using DMA (%)
20	13.15	3.89	2.72
40	65.1	24.51	19.96
60	92.045	46.75	40.1
80	99.025	65.42	57.3
100	99.67	79.05	70.77
120	100	87.5	80.52
140	100	93.01	87.5
160	100	96.6	92.37

Table 9. Impact of the number of fibers on the SO₂ separation performance using seawater, NaOH and DMA liquid absorbents.

Data availability

All data generated or analyzed during this study are included in this published article.

Received: 27 August 2022; Accepted: 20 January 2023

Published online: 24 January 2023

References

- Rahmani, F., Mowla, D., Karimi, G., Golkhar, A. & Rahmatmand, B. SO₂ removal from simulated flue gas using various aqueous solutions: Absorption equilibria and operational data in a packed column. *Sep. Purif. Technol.* **153**, 162–169 (2015).
- Shirazian, S., Taghvaie Nakhjiri, A., Heydarinasab, A. & Ghadiri, M. Theoretical investigations on the effect of absorbent type on carbon dioxide capture in hollow-fiber membrane contactors. *PLoS ONE* **15**, e0236367 (2020).
- Cao, Y., Taghvaie Nakhjiri, A. & Ghadiri, M. CFD investigation of CO₂ separation from anesthesia gaseous stream applying novel cholinium lysinate amino acid-based ionic liquid inside the gas-liquid membrane contactor. *Eur. Phys. J. Plus* **137**, 1044 (2022).
- Fioletov, V. E. *et al.* A global catalogue of large SO₂ sources and emissions derived from the ozone monitoring instrument. *Atmos. Chem. Phys.* **16**, 11497–11519 (2016).
- Pishnamazi, M. *et al.* Computational study on SO₂ molecular separation applying novel EMISE ionic liquid and DMA aromatic amine solution inside microporous membranes. *J. Mol. Liq.* **313**, 113531 (2020).
- Brogren, C. & Karlsson, H. T. Modeling the absorption of SO₂ in a spray scrubber using the penetration theory. *Chem. Eng. Sci.* **52**, 3085–3099 (1997).

7. Park, H. J. *et al.* Experimental study on the selective removal of SO₂ from a ship exhaust gas stream using a membrane contactor. *Ind. Eng. Chem. Res.* **58**, 14897–14905 (2019).
8. Sun, X., Meng, F. & Yang, F. Application of seawater to enhance SO₂ removal from simulated flue gas through hollow fiber membrane contactor. *J. Membr. Sci.* **312**, 6–14 (2008).
9. Nakhjiri, A. T. & Heydarinasab, A. CFD analysis of CO₂ sequestration applying different absorbents inside the microporous PVDF hollow fiber membrane contactor. *Period. Polytech. Chem. Eng.* **64**, 135–145 (2020).
10. Drioli, E., Curcio, E. & Di Profio, G. State of the art and recent progresses in membrane contactors. *Chem. Eng. Res. Des.* **83**, 223–233 (2005).
11. Nakhjiri, A. T., Heydarinasab, A., Bakhtiari, O. & Mohammadi, T. Modeling and simulation of CO₂ separation from CO₂/CH₄ gaseous mixture using potassium glycinate, potassium arginate and sodium hydroxide liquid absorbents in the hollow fiber membrane contactor. *J. Environ. Chem. Eng.* **6**, 1500–1511 (2018).
12. Rongwong, W. *et al.* Investigation of the effects of operating parameters on the local mass transfer coefficient and membrane wetting in a membrane gas absorption process. *J. Membr. Sci.* **490**, 236–246 (2015).
13. Cao, Y. *et al.* Mathematical modeling and numerical simulation of CO₂ capture using MDEA-based nanofluids in nanostructure membranes. *Process Saf. Environ. Prot.* **148**, 1377–1385 (2021).
14. Cao, Y. *et al.* Recent advancements in molecular separation of gases using microporous membrane systems: A comprehensive review on the applied liquid absorbents. *J. Mol. Liq.* **337**, 116439 (2021).
15. Mansourizadeh, A., Aslmahdavi, Z., Ismail, A. & Matsuura, T. Blend polyvinylidene fluoride/surface modifying macromolecule hollow fiber membrane contactors for CO₂ absorption. *Int. J. Greenh. Gas Control* **26**, 83–92 (2014).
16. Nakhjiri, A. T., Heydarinasab, A., Bakhtiari, O. & Mohammadi, T. Experimental investigation and mathematical modeling of CO₂ sequestration from CO₂/CH₄ gaseous mixture using MEA and TEA aqueous absorbents through polypropylene hollow fiber membrane contactor. *J. Membr. Sci.* **565**, 1–13 (2018).
17. Nakhjiri, A. T., Heydarinasab, A., Bakhtiari, O. & Mohammadi, T. The effect of membrane pores wettability on CO₂ removal from CO₂/CH₄ gaseous mixture using NaOH, MEA and TEA liquid absorbents in hollow fiber membrane contactor. *Chin. J. Chem. Eng.* **26**, 1845–1861 (2018).
18. Marjani, A., Nakhjiri, A. T., Pishnamazi, M. & Shirazian, S. Evaluation of potassium glycinate, potassium lysinate, potassium sarcosinate and potassium threonate solutions in CO₂ capture using membranes. *Arab. J. Chem.* **14**, 102979 (2021).
19. Henares, M., Ferrero, P., San-Valero, P., Martinez-Soria, V. & Izquierdo, M. Performance of a polypropylene membrane contactor for the recovery of dissolved methane from anaerobic effluents: Mass transfer evaluation, long-term operation and cleaning strategies. *J. Membr. Sci.* **563**, 926–937 (2018).
20. Park, H. H., Deshwal, B. R., Kim, I. W. & Lee, H. K. Absorption of SO₂ from flue gas using PVDF hollow fiber membranes in a gas-liquid contactor. *J. Membr. Sci.* **319**, 29–37 (2008).
21. Ahn, Y., Hwang, Y.-H. & Shin, H.-S. Application of PTFE membrane for ammonia removal in a membrane contactor. *Water Sci. Technol.* **63**, 2944–2948 (2011).
22. Marjani, A., Nakhjiri, A. T., Adimi, M., Jirandehi, H. F. & Shirazian, S. Effect of graphene oxide on modifying polyethersulfone membrane performance and its application in wastewater treatment. *Sci. Rep.* **10**, 1–11 (2020).
23. Cao, Y., Nakhjiri, A. T. & Ghadiri, M. Membrane desalination for water treatment: recent developments, techno-economic evaluation and innovative approaches toward water sustainability. *Eur. Phys. J Plus* **137**, 763 (2022).
24. Mansourizadeh, A. & Ismail, A. Hollow fiber gas-liquid membrane contactors for acid gas capture: A review. *J. Hazard. Mater.* **171**, 38–53 (2009).
25. Hu, H. H. Chapter 10—Computational fluid dynamics. In *Fluid Mechanics (5th Edition)* (eds Kundu, P. K. *et al.*) 421–472 (Academic Press, 2012).
26. Pishnamazi, M., Nakhjiri, A. T., Taleghani, A. S., Marjani, A., Heydarinasab, A., & Shirazian, S. Computational investigation on the effect of [Bmim][BF₄] ionic liquid addition to MEA alkanolamine absorbent for enhancing CO₂ mass transfer inside membranes. *J. Mol. Liq.* **314**, 113635 (2020).
27. Babanezhad, M., Taghvaei Nakhjiri, A., Rezakazemi, M., & Shirazian, S. Developing intelligent algorithm as a machine learning overview over the big data generated by Euler–Euler method to simulate bubble column reactor hydrodynamics. *ACS omega*, **5**, 20558–20566 (2020).
28. Shen, R., Jiao, Z., Parker, T., Sun, Y. & Wang, Q. Recent application of computational fluid dynamics (CFD) in process safety and loss prevention: A review. *J. Loss Prev. Process Ind.* **67**, 104252 (2020).
29. Babanezhad, M. *et al.* High-performance hybrid modeling chemical reactors using differential evolution based fuzzy inference system. *Sci. Rep.* **10**, 1–11 (2020).
30. Dixon, A. G. & Partopour, B. Computational fluid dynamics for fixed bed reactor design. *Annu. Rev. Chem. Biomol. Eng.* **11**, 109–130 (2020).
31. Nakhjiri, A. T. & Roudsari, M. H. Modeling and simulation of natural convection heat transfer process in porous and non-porous media. *Appl. Res. J* **2**, 199–204 (2016).
32. Nakhjiri, A. T. & Heydarinasab, A. Computational simulation and theoretical modeling of CO₂ separation using EDA, PZEA and PS absorbents inside the hollow fiber membrane contactor. *J. Ind. Eng. Chem.* **78**, 106–115 (2019).
33. Zawawi, M. H., Saleha, A., Salwa, A., Hassan, N., Zahari, N. M., Ramli, M. Z., Muda, Z. C. A review: Fundamentals of computational fluid dynamics (CFD) In: *AIP Conf. Proc.* (AIP Publishing LLC, NY, 2018) pp. 020252.
34. Cao, Y., Nakhjiri, A. T., Sarkar, S. M. & Ghadiri, M. Time-dependent numerical investigation of 3-hydroxypropionic acid extraction using a microporous membrane contactor. *Eur. Phys. J. Plus* **137**, 1–9 (2022).
35. Pozzobon, V. & Perré, P. Mass transfer in hollow fiber membrane contactor: Computational fluid dynamics determination of the shell side resistance. *Sep. Purif. Technol.* **241**, 116674 (2020).
36. Haghshenasfard, M., Moheb, A. & Ansari-pour, M. Application of computational fluid dynamics technique in membrane contactor systems. In *Current Trends and Future Developments on (Bio-) Membranes* 289–310 (Elsevier, Amsterdam, 2022).
37. Nakhjiri, A. T. & Heydarinasab, A. Efficiency evaluation of novel liquid potassium lysinate chemical solution for CO₂ molecular removal inside the hollow fiber membrane contactor: Comprehensive modeling and CFD simulation. *J. Mol. Liq.* **297**, 111561 (2020).
38. Ariono, D., Hakim, A. & Wenten, I. Experimental investigation and numerical analysis of SO₂ removal using polypropylene membrane contactor. *J. Phys. Conf. Ser. IOP Pub.* **1090**, 012008 (2018).
39. Kong, X. *et al.* Mass-transfer characteristics and optimization of a hydrophilic ceramic membrane contactor for SO₂ absorption. *Ind. Eng. Chem. Res.* **58**, 20828–20837 (2019).
40. File:Water-3D-balls-A.png. (2020, September 14). Wikimedia Commons, the free media repository. Retrieved 09:00, August 19, 2022 from <https://commons.wikimedia.org/w/index.php?title=File:Water-3D-balls-A.png&oldid=459003747>.
41. Wikipedia contributors. (2022, January 1). Dimethylaniline. In Wikipedia, The Free Encyclopedia. Retrieved 08:47, August 19, 2022, from <https://en.wikipedia.org/w/index.php?title=Dimethylaniline&oldid=1063135665>.
42. Wikipedia contributors. (2022, August 12). Sodium hydroxide. In Wikipedia, The Free Encyclopedia. Retrieved 08:49, August 19, 2022, from https://en.wikipedia.org/w/index.php?title=Sodium_hydroxide&oldid=1104073985.
43. Water Science and Technology Library. *Marine Chemistry. An Analytical Environmental Chemistry Approach. Water Science and Technology Library* Vol. 25, 407 (Kluwer Academic Publisher, Dordrecht, 1997).

44. Nakhjiri, A. T., Sanaeepur, H., Amooghini, A. E. & Shirazi, M. M. A. Recovery of precious metals from industrial wastewater towards resource recovery and environmental sustainability: A critical review. *Desalination* **527**, 115510 (2022).
45. Bhattacharya, S., Dutta, B. K., Shyamal, M. & Basu, R. K. Absorption of sulfur dioxide in aqueous dispersions of dimethyl aniline. *Can. J. Chem. Eng.* **74**, 339–346 (1996).
46. Basu, R. K. & Dutta, B. K. Kinetics of absorption of sulfur dioxide in dimethylaniline solution. *Can. J. Chem. Eng.* **65**, 27–35 (1987).
47. Chang, C. S. *Mass Transfer with Equilibrium Chemical Reaction, Sulphur-dioxide Absorption in Aqueous Solutions* (University of Texas, Austin, 1980).
48. Bazhenov, S. D., Bilydyukovich, A. V. & Volkov, A. V. Gas-liquid hollow fiber membrane contactors for different applications. *Fibers* **6**, 76 (2018).
49. Qi, Z. & Cussler, E. Microporous hollow fibers for gas absorption: I. Mass transfer in the liquid. *J. Membr. Sci.* **23**, 321–332 (1985).
50. Gabelman, A. & Hwang, S.-T. Hollow fiber membrane contactors. *J. Membr. Sci.* **159**, 61–106 (1999).
51. Rasaie, M., Elhambakhsh, A., Eskandari, M., Keshavarz, P. & Mowla, D. Highly selective physical/chemical CO₂ separation by functionalized Fe₃O₄ nanoparticles in hollow fiber membrane contactors: Experimental and modeling approaches. *Energy Fuels* **36**, 4456–4469 (2022).
52. Zhang, Z. Comparisons of various absorbent effects on carbon dioxide capture in membrane gas absorption (MGA) process. *J. Nat. Gas Sci. Eng.* **31**, 589–595 (2016).
53. Zhang, Z., Yan, Y., Zhang, L., Chen, Y. & Ju, S. CFD investigation of CO₂ capture by methyl-diethanolamine and 2-(1-piperazinyl)-ethylamine in membranes: Part B. Effect of membrane properties. *J. Nat. Gas Sci. Eng.* **19**, 311–316 (2014).
54. Al-Marzouqi, M., El-Naas, M., Marzouk, S. & Abdullatif, N. Modeling of chemical absorption of CO₂ in membrane contactors. *Sep. Purif. Technol.* **62**, 499–506 (2008).
55. Ghadiri, M., Mohammadi, M., Asadollahzadeh, M. & Shirazian, S. Molecular separation in liquid phase: Development of mechanistic model in membrane separation of organic compounds. *J. Mol. Liq.* **262**, 336–344 (2018).
56. Pishnamazi, M. *et al.* Computational fluid dynamics simulation of NO₂ molecular sequestration from a gaseous stream using NaOH liquid absorbent through porous membrane contactors. *J. Mol. Liq.* **313**, 113584 (2020).
57. Nguyen, Q., Babanezhad, M., Taghvaei Nakhjiri, A., Rezakazemi, M. & Shirazian, S. Prediction of thermal distribution and fluid flow in the domain with multi-solid structures using cubic-interpolated pseudo-particle model. *PLoS ONE* **15**, e0233850 (2020).
58. Cao, Y. *et al.* Intensification of CO₂ absorption using MDEA-based nanofluid in a hollow fibre membrane contactor. *Sci. Rep.* **11**, 1–12 (2021).
59. Pishnamazi, M. *et al.* Molecular investigation into the effect of carbon nanotubes interaction with CO₂ in molecular separation using microporous polymeric membranes. *Sci. Rep.* **10**, 1–12 (2020).
60. Bird, R. B. Transport phenomena. *Appl. Mech. Rev.* **55**, R1–R4 (2002).
61. Nakhjiri, A. T., Heydarinasab, A., Bakhtiari, O. & Mohammadi, T. Influence of non-wetting, partial wetting and complete wetting modes of operation on hydrogen sulfide removal utilizing monoethanolamine absorbent in hollow fiber membrane contactor. *Sustain. Environ. Res.* **28**, 186–196 (2018).
62. Babanezhad, M., Masoumian, A., Nakhjiri, A. T., Marjani, A. & Shirazian, S. Influence of number of membership functions on prediction of membrane systems using adaptive network based fuzzy inference system (ANFIS). *Sci. Rep.* **10**, 1–20 (2020).
63. Karoor, S. & Sirkar, K. K. Gas absorption studies in microporous hollow fiber membrane modules. *Ind. Eng. Chem. Res.* **32**, 674–684 (1993).
64. Luis, P., Garea, A. & Irabien, A. Modelling of a hollow fibre ceramic contactor for SO₂ absorption. *Sep. Purif. Technol.* **72**, 174–179 (2010).
65. Faiz, R. & Al-Marzouqi, M. Mathematical modeling for the simultaneous absorption of CO₂ and H₂S using MEA in hollow fiber membrane contactors. *J. Membr. Sci.* **342**, 269–278 (2009).
66. Dutta, B. K., Basu, R. K., Pandit, A. & Ray, P. Absorption of sulfur dioxide in citric acid-sodium citrate buffer solutions. *Ind. Eng. Chem. Res.* **26**, 1291–1296 (1987).
67. Luis, P., Garea, A. & Irabien, A. Zero solvent emission process for sulfur dioxide recovery using a membrane contactor and ionic liquids. *J. Membr. Sci.* **330**, 80–89 (2009).
68. Chang, C.-S. & Rochelle, G. T. SO₂ absorption into NaOH and Na₂SO₃ aqueous solutions. *Ind. Eng. Chem. Fundam.* **24**, 7–11 (1985).
69. Hikita, H., Asai, S. & Tsuji, T. Absorption of sulfur dioxide into aqueous sodium hydroxide and sodium sulfite solutions. *AIChE J.* **23**, 538–544 (1977).
70. Koonaphaddeert, S., Wu, Z. & Li, K. Carbon dioxide stripping in ceramic hollow fibre membrane contactors. *Chem. Eng. Sci.* **64**, 1–8 (2009).
71. Vázquez, G., Antorrena, G., Chenlo, F. & Paleo, F. Absorption of SO₂ by aqueous NaOH solutions in the presence of a surfactant. *Chem. Eng. Technol.* **11**, 156–162 (1988).
72. Xu, P. *et al.* Hydrophilic membrane contactor for improving selective removal of SO₂ by NaOH solution. *Sep. Purif. Technol.* **250**, 117134 (2020).

Author contributions

Y.C.: Modelling, formal analysis, writing original draft; A.T.N.: Writing original draft, validation, resources, software, reviewing and editing, data curation; M.G.: Methodology, conceptualization, resources, reviewing and editing, supervision, project administration.

Funding

The work submitted for publication did not receive financial support from anyone. No researchers other than the author participated in it.

Competing interests

The authors declare no competing interests.

Additional information

Correspondence and requests for materials should be addressed to A.T.N.

Reprints and permissions information is available at www.nature.com/reprints.

Publisher's note Springer Nature remains neutral with regard to jurisdictional claims in published maps and institutional affiliations.



Open Access This article is licensed under a Creative Commons Attribution 4.0 International License, which permits use, sharing, adaptation, distribution and reproduction in any medium or format, as long as you give appropriate credit to the original author(s) and the source, provide a link to the Creative Commons licence, and indicate if changes were made. The images or other third party material in this article are included in the article's Creative Commons licence, unless indicated otherwise in a credit line to the material. If material is not included in the article's Creative Commons licence and your intended use is not permitted by statutory regulation or exceeds the permitted use, you will need to obtain permission directly from the copyright holder. To view a copy of this licence, visit <http://creativecommons.org/licenses/by/4.0/>.

© The Author(s) 2023